Removal of methyl orange from aqueous solution by heterogeneous Electro-Fenton process using $MnFe_2O_4$/C catalyst

Pham Hong Tuan[1*], Nguyen Van Dung[1], Nguyen Nhat Huy[2], Le Anh Kien[1]

[1]Institute for Tropical Technology, Academy Science and Technology, 57A Truong Quoc Dung Street, Phu Nhuan, Ho Chi Minh City, Vietnam;
[2]Faculty of Environment and Natural Resources, Ho Chi Minh City University of Technology, 268 Ly Thuong Kiet, Dien Hong, Ho Chi Minh City, Vietnam.
[*]Corresponding author: tuan140482@gmail.com
Received 12 Aug. 2025; Revised 8 Oct. 2025; Accepted 10 Nov. 2025; Published 28 Nov. 2025.
DOI: https://doi.org/10.54939/1859-1043.j.mst.107.2025.68-77

ABSTRACT

In this study, the heterogeneous Electro-Fenton process using a manganese ferrite catalyst on activated carbon derived from sugarcane bagasse ($MnFe_2O_4$/C) was investigated for the removal of methyl orange (MO) dye from aqueous solution. $MnFe_2O_4$/C was synthesized by an impregnation-coprecipitation method and characterized by scanning electron microscopy (SEM), energy dispersive X-ray spectrometer (EDS), X-ray diffraction (XRD). Electro-Fenton model using graphite electrodes. The experiment was carried out to examine the efficiency of MO removal under neutral pH conditions. The effect of various operational parameters, such as applied current, catalyst loading, initial methyl orange concentration, was investigated.

Keywords: Heterogeneous Electro-Fenton; Methyl orange; Manganese Ferrite/Activated carbon.

1. INTRODUCTION

Azo dyes with one or more azo bonds (–N=N–) in association with one or more aromatic rings are a kind of synthetic dye that is most widely used in the dyeing process of textile industries. It has been estimated that more than 50% of all dyes are azo dyes due to their chemical stability and versatility. Azo dyes in wastewater are persistent and difficult to biodegrade compounds due to their highly structured polymeric nature [1, 2]. The removal of azo dyes from wastewater by biological and conventional chemical treatments is a challenge to the textile industries because of their toxicity and stability. Dyeing wastewater discharged into the aquatic environment will be harmful to both aquatic organisms and humans due to toxic, carcinogenic and mutagenic effects [3]. Methyl orange (MO) is a typical azo dye that is generally used as a colouring agent in the textile and leather industries. It is widely used in printing, paper manufacturing, pharmaceutical, food processing industries, and in research laboratories. MO is a carcinogenic water-soluble azo dye, and is also acknowledged as an acidic or anionic dye. It can cause vomiting and diarrhea. High levels of exposure to MO can result in death. It is also metabolised into aromatic amines by intestinal microorganisms. Methyl orange is stable, shows low biodegradability and is soluble in water; hence, it is difficult to remove from aqueous solutions by common water purification or treatment methods [4-6].

Wastewater treatment techniques, including membrane filtration, ion exchange, coagulation, advanced oxidation processes, biological processes, and adsorption, were used for the removal of dyes [3, 7]. Advanced oxidation processes (AOPs) are a suitable method for the treatment of persistent organic pollutants [8]. AOPs are based on the *in situ* generation of hydroxyl radicals (•OH), a highly reactive (oxidation potential: 2.8 V) and non-selectively decomposes many types of organic substances. Among them, Electro-Fenton (EF) is one of the technologies that is currently being studied due to its fast reaction rate, low toxicity and environmental friendly. During the EF process, H_2O_2 is generated at the cathode surface via oxygen reduction reaction (ORR) and reacts with iron catalyst (Fe^{2+}) to produce •OH and degrade pollutants.

$$O_2 + 2H^+ + 2e^- \rightarrow H_2O_2 \quad (1)$$

$$Fe^{2+} + H_2O_2 \rightarrow Fe^{3+} + \bullet OH + OH^- \quad (2)$$

$$\bullet OH + \text{pollutants} \rightarrow \text{by products} \rightarrow CO_2 + H_2O \quad (3)$$

The heterogeneous electro-Fenton (HEF) process is carried out with a solid Fe-containing catalyst, which reacts with H_2O_2 to form •OH, promoting mineralization and efficient removal of pollutants. This process has several advantages, such as a wider pH range for the Fenton reaction (even possible under alkaline pH conditions), prevention of leaching of iron ions, increased stability and reusability of the catalyst, and inhibition of iron hydroxide precipitation, resulting in a reduction in secondary sludge [9]. Iron oxides are considered environmentally acceptable Fenton catalysts, as they are abundant in nature and are easy to synthesize, making them low-cost. Recently, various transition metals such as cobalt (Co), copper (Cu), nickel (Ni) and manganese (Mn) have been utilized as solid catalysts with iron/iron oxides. Adding transition metals such as Cu, Mn and Ni to Fe_3O_4 was reported to be effective for the increased catalytic activity [10]. Various methods can be used to synthesize $MnFe_2O_4$, such as mechanochemical reaction, sol-gel, hydrothermal, soft chemical route, solid combustion route, microwave combustion, solvothermal, co-precipitation. The co-precipitation method is often used to synthesize multi-metal oxides because it is simple, and the obtained material is more [11].

Manganese ferrite ($MnFe_2O_4$) catalyst has attracted more attention due to its large surface area and high surface activity [12]. $MnFe_2O_4$ nanoparticles have significant advantages, such as good catalytic activity, easy synthesis, simple operation, environmentally friendly, and can be separated from the reaction medium after being magnetized by an external magnet [13]. Mn and Fe ions have been used as heterogeneous catalysts in the $MnFe_2O_4/H_2O_2$ system, where manganese ferrite ($MnFe_2O_4$) nanoparticles have considerable stability in the catalytic process due to their unique spinel crystal structure [14]. $MnFe_2O_4$ nanoparticles are also magnetic materials that can easily be separated from an aqueous solution by an external magnetic field, providing an attractive and cost-effective method for practical operation. However, these catalysts have a limited catalytic performance due to their easy agglomeration. Therefore, it is necessary to find a suitable carrier to improve the catalytic performance of these materials while avoiding agglomeration.

Carbon, especially activated carbon, is a well-known adsorbent widely used for the removal of dyes, heavy metals, phenols, pesticides, etc. Higher surface area, sorption capacity, porosity, etc. of activated carbon made the material as popular adsorbent. The ability of activated carbon for the sorption of heavy metals leads to the preparation of an activated carbon-supported iron catalyst for the abatement of various organic pollutants via Fenton's reaction [15]. Activated carbon is a good carrier material that can inhibit the aggregation of metal oxides.

In the solution and on the surface of the catalyst containing Fe and Mn. The reactions to create free hydroxyl radicals (•OH) will take place as follows:

$$\equiv Fe^{II} + H_2O_2 \rightarrow \equiv Fe^{III} + \bullet OH + OH^- \quad (4)$$

$$\equiv Mn^{II} + H_2O_2 \rightarrow \equiv Mn^{III} + \bullet OH + OH^- \quad (5)$$

$\equiv Fe^{III}$ and $\equiv Mn^{III}$ are electrochemically reduced to $\equiv Fe^{II}$ and $\equiv Mn^{II}$ in the electrolyte environment through electron acceptance and continue to react with H_2O_2 according to equations (6) and (7) to produce •OH as a continuous cycle.

$$\equiv Fe^{III} + e^- \rightarrow Fe^{II} \quad (6)$$

$$\equiv Mn^{III} + e^- \rightarrow \equiv Mn^{II} \quad (7)$$

In this study, $MnFe_2O_4$/C catalyst material was synthesized by the impregnation-coprecipitation method and used for the electro-Fenton process to remove MO in aqueous solution.

2. MATERIALS AND METHODS

2.1. Materials and chemicals

Activated carbon was prepared from sugarcane bagasse biomass in Viet Nam. Chemicals employed in the synthesis of $MnFe_2O_4$/C and experiments include potassium hydroxide (KOH, 96%, XiLong-China), manganese (II) chloride tetrahydrate ($MnCl_2.4H_2O$, 99%, Xilong-China), ferric chloride hexahydrate ($FeCl_3.6H_2O$, 99%, Xilong–China), ammonia solution (NH_3, 25%, Xilong-China), methyl orange (MO) ($C_{14}H_{14}N_3NaO_3S$, 99%, Xilong-China).

2.2. Preparation of $MnFe_2O_4$/C composite

Activated carbon was prepared from bagasse biomass. The bagasse was collected after juice extraction, and impurities on its surface were removed with clean water. It was then dried at 80 ºC for 2 hours and cut into small pieces. Next, the bagasse was soaked in a KOH solution (1:1 ratio by mass), with the temperature stabilized at 70 ºC using a thermostatic bath for 2 hours. It was then separfiltered and dried at 80 ºC for 10 hours. The bagasse was carbonized at 700 ºC for 2 hours at a heating rate of 5 ºC/min (in an airtight environment). Finally, the activated carbon was washed with distilled water until reaching a neutral pH and dried at 80 ºC for 8 hours.

The $MnFe_2O_4$/C composite was synthesized through the impregnation-coprecipitation method. The typical synthesis process was described as follows: dissolving 1.78 g of $MnCl_2.4H_2O$ and 4.85 g of $FeCl_3.6H_2O$ in 100 mL of deionized water. Then, 5.0 g of activated carbon (prepared from bagasse biomass) was added to the above mixed solutions and stirred for 60 min. Subsequently, an ammonia solution (NH_3) was added drop-wise into the suspensions, stirred for 120 min at 70 ºC (using a thermostatic water bath). Afterward, the solution was cooled down to room temperature, the $MnFe_2O_4$/C composite was separated and washed with ethanol and distilled water until the pH reached the neutral region. The composite was then dried in an oven at 80 ºC for 8 h. Finally, the dried composite was pyrolyzed at 700 ºC for 1 h in the presence of nitrogen to form the maganese ferrite/activated carbon material ($MnFe_2O_4$/C).

2.3. Characterization of $MnFe_2O_4$/C material

The surface morphologies and element contents of material was obtained by a scanning electron microscopy (SEM) equipped with energy dispersive spectrometer (EDS) (JSM IT 200, Jeol – Japan), Investigate the crystal structure of the material by X-ray diffraction (XRD) (D2 Phaser, Bruker-Germany), The specific surface area was analyzed using the nitrogen adsorption/desorption method at 77,35 K (BET-201A, PMI-USA).

2.4. The experimental procedure

The experimental model was set up, including a DC power supply (PS40-30A, TEXIO), two pairs of graphite electrodes (10 cm × 5 cm) with a distance of 2 cm apart, 1.000 ml beaker as the reactor. The simulation wastewater containing MO was prepared by dissolving MO powder into tap water. Na_2SO_4 (0.0025 mol/L) was added to create an electrolyte environment. $MnFe_2O_4$/C material was employed as the particle catalyst for the heterogenous electro-Fenton process. The solution was continuously stirred by a magnetic stirrer to maintain a uniform concentration of the electrolyte solution. During the experiments, a certain amount of solution was extracted from the reactor periodically for MO analysis. Samples were analyzed immediately after filtration through 0.45 μm membrane filters to remove suspended particles.

The concentration of MO was analyzed on a UV–vis spectrophotometer (XD7000, Lovibond-Germany) at the wavelength of λ = 464 nm [16]. Methyl orange degradation efficiency is determined by using the following expression:

$$H\% = \left(1 - \frac{C_t}{C_0}\right) \times 100\%$$

Where, C_t and C_0 are the concentrations at the sampling time and the initial concentration of methyl orange, respectively.

$$-\frac{d[C_{(MO)}]}{dt} = k[\bullet OH] \times C_{(MO)} = k_{app} \times C_{(MO)}$$

With $k_{app} = k[\bullet OH]$ determined from experimental data by plotting graph $-\ln(C_t/C_o)$ vs reaction time t (min) when $R^2 > 0.99$.

3. RESULTS AND DISCUSSION

3.1. Characteristics of the $MnFe_2O_4$/C material

The surface morphology of activated carbon and $MnFe_2O_4$/C composite samples was determined by scanning electron microscopy (SEM) with a maximum magnification of 5,000 times. SEM images (figure 1) have shown that the surface morphology of the $MnFe_2O_4$/C sample compared to activated carbon samples (C) has a clearly difference. The original activated carbon sample has a smooth surface with numerous pores. The $MnFe_2O_4$/C composite (modified with a mixture of Mn^{2+} and Fe^{3+} metal salts) has a rough surface and fewer pores. This occurs because metal oxide particles are randomly distributed on the surface and in the pores.

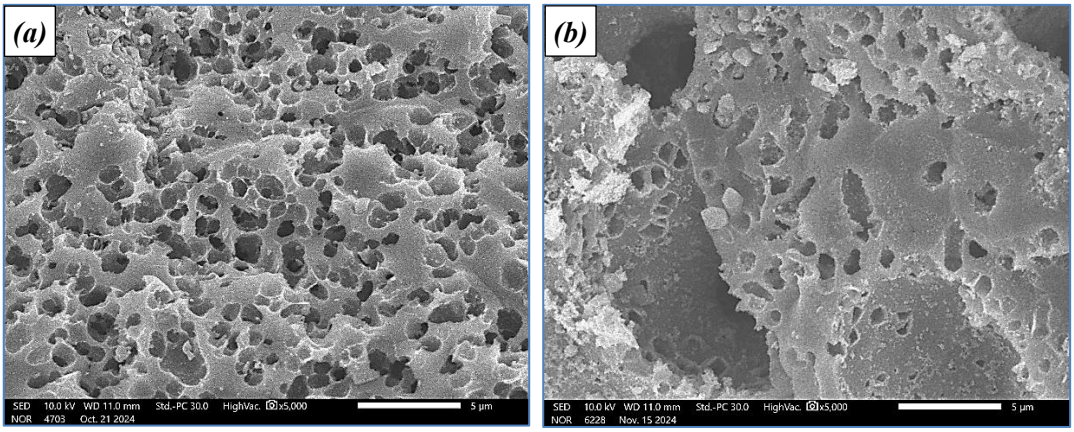

Figure 1. *SEM of activated carbon (a) and $MnFe_2O_4$/C (b).*

The results of EDS analysis show that activated carbon contains major elements of carbon (82.98 %), oxygen (10.87 %) and potassium (5.03%). The addition of $MnFe_2O_4$ to the activated carbon causes a decrease in carbon content (35.88%) and an increase in O (19.91%), Fe (30.21%), and Mn (11,29%). This proves that the composite synthesis process has been successful. This result can predict the appearance of Mn-O, Fe-O bonds in the cubic crystal structure of $MnFe_2O_4$.

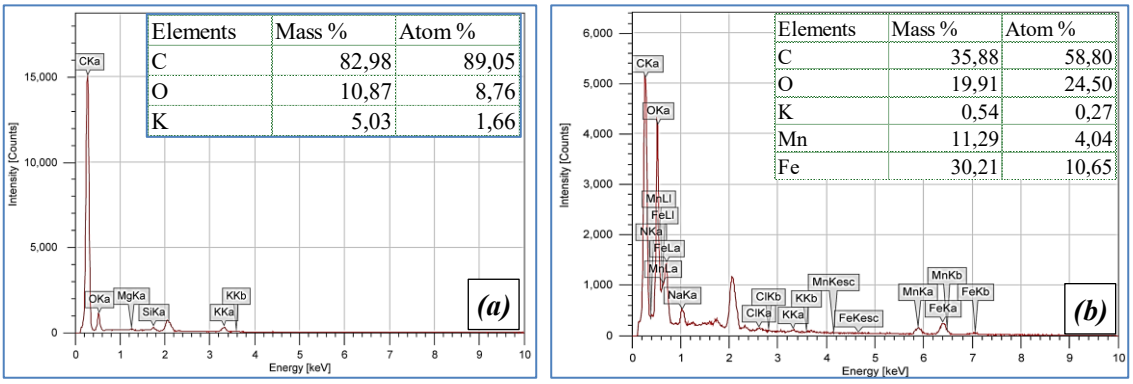

Figure 2. *EDS analysis of activated carbon (a) and $MnFe_2O_4$/C (b).*

The SEM and EDS data are consistent with the BET specific surface area data for the two material samples. The N_2 adsorption-desorption isotherms (figure 3) show that the adsorption capacity of activated carbon is higher than that of $MnFe_2O_4$/C due to the higher specific surface area, pore volume, and especially the average mesopore volume of the activated carbon compared to $MnFe_2O_4$/C. The $MnFe_2O_4$/C sample exhibits a significantly reduced specific surface area (324.396 m^2/g) compared to the activated carbon sample (639.046 m^2/g). This reduction is attributed to the adsorption and bonding of $MnFe_2O_4$ onto both the surface and within the pores of the activated carbon. The occupation of the activated carbon's pores by $MnFe_2O_4$ nanoparticles led to a significant decrease in the total pore volume of the activated carbon (0.3832 cm^3/g) after the successful bonding of $MnFe_2O_4$ (0.2347 cm^3/g).

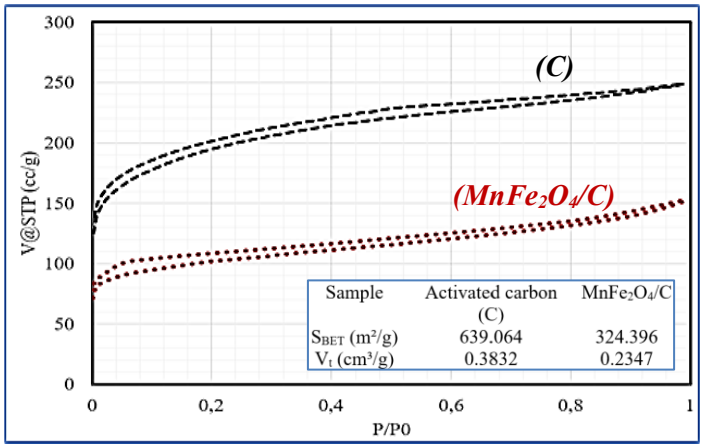

Figure 3. *N_2 adsorption – desorption isotherm.*

The XRD pattern of the $MnFe_2O_4$/C sample shows characteristic peaks for the (hkl) planes of the $MnFe_2O_4$ crystal structure at 2θ angles of 29.70°, 34.98°, 42.52°, 56.19°, and 61.65°, corresponding to the crystal planes of spinel ferrite (220), (311), (400), (511), and (440), respectively [17]. This indicates that $MnFe_2O_4$ nanoparticles were successfully immobilized onto the activated carbon using the impregnation-coprecipitation method. The $MnFe_2O_4$/C material was also tested for magnetism using a magnet. $MnFe_2O_4$/C was attracted to the magnet due to its magnetic properties, making it very easy to separate and reuse the catalyst after the reaction.

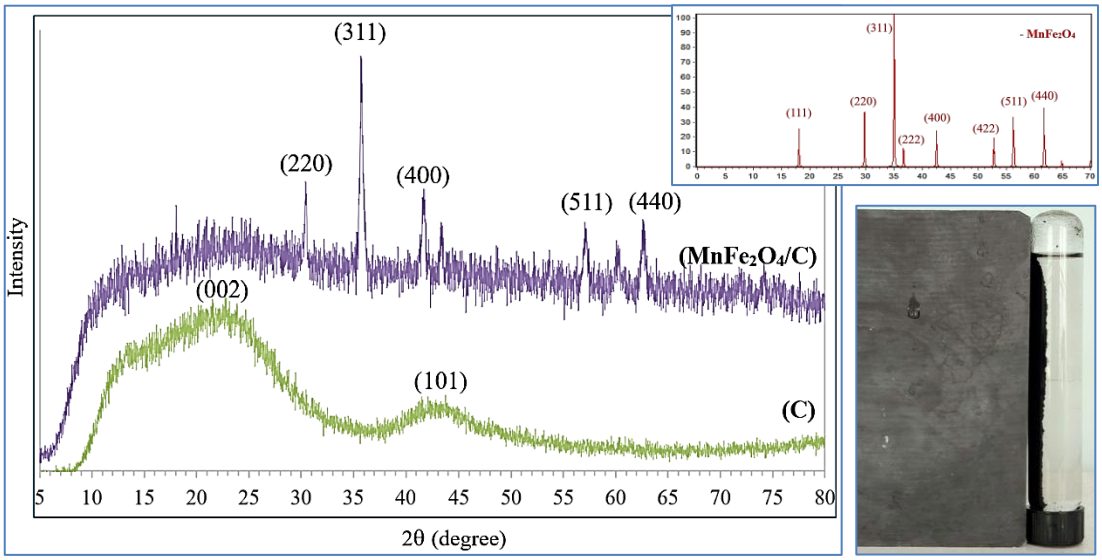

Figure 4. *XRD patterns of $MnFe_2O_4$/C and activated carbon (C).*

3.2. Methyl orange removal efficiency by HEF

Experiments were conducted to evaluate the efficiency of MO removal by the HEF process using an $MnFe_2O_4$ catalyst under neutral pH conditions (pH ranging from 6.8 to 7.1). 0.0025 mol/L Na_2SO_4 was added to the solution as electrolyte in all experiments.

3.2.1. Effect of current density

The experiment was performed with current density from 0.5 mA/cm² to 5 mA/cm², initial MO concentration of 100 ppm. The results showed that MO removal efficiency increased with increasing current density and achieved the best result at 3 mA/cm². MO removal efficiency reached approximately 93% with 120 minutes of reaction corresponding to MO degradation rate constant K(3.0)=2.21 x 10^{-2} (min^{-1}). Increasing the current density to 5 mA/cm², the MO removal efficiency was almost similar to 3 mA/cm² (about 95%, 120 minutes of reaction). On the other hand, in the experiment without applying current density (J=0.00 mA/cm²), the MO removal efficiency was only about 14%, due to the MO adsorption effect of $MnFe_2O_4$/C material. Thereby, it can be confirmed that MO removal is effective by the electro-Fenton process. The MO removal efficiency under neutral pH conditions using the HEF process was significantly higher than that of the conventional heterogeneous Fenton process with Fe_2MnO_4/AC and Fe_3O_4/AC (AC: activated carbon), which achieved only 28% and 19% removal after 120 minutes, respectively [18].

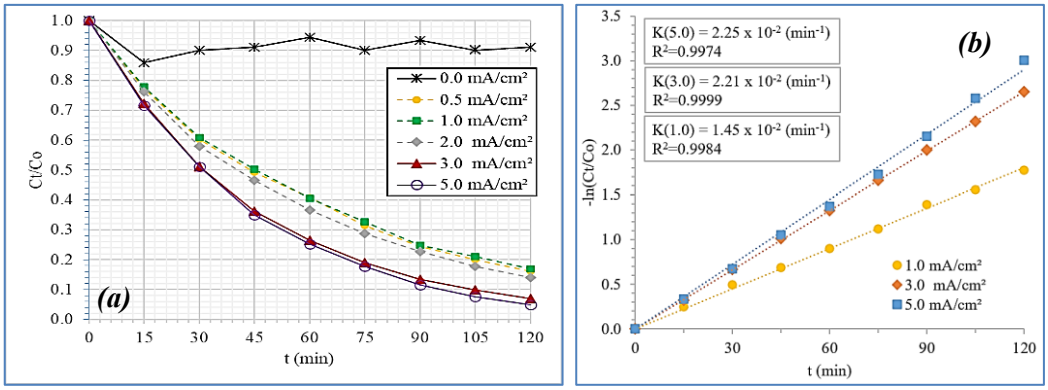

Figure 5. *Effect of current density (4a); $ln(C_o/C_t)$ v.s time (4b).*

From figure 5b, it can be seen that the kinetics of MO removal via the HEF process follow a pseudo-first-order kinetic model with a regression coefficient $R^2 \geq 0.99$. The apparent rate constant increases correspondingly to the applied current density in the experiment.

Current intensity is considered to be the main factor influencing the generation of hydroxyl radicals •OH according to equations (1) and (4) - (7). At low current densities, H_2O_2 generation occurs under controlled electron transfer conditions. Therefore, increasing the current increases the charge distribution across the cathode, leading to an increase in the concentration of hydroxyl radicals in the solution. However, the excessive current can promote side reactions such as the decomposition of H_2O_2 (equation (8)) and the reduction of the generated H^+ ions to H_2 (equation (9)) [19]. Increasing the current density to 5 mA/cm² can slow down the production of H_2O_2 and promote the H_2 formation reaction at the cathode (competing with the formation of H_2O_2 according to equation (1), leading to the MO removal efficiency not increasing correspondingly with the current density.

$$H_2O_2 + 2H^+ + 2e^- \rightarrow 2H_2O \quad (8)$$

$$2H^+ + 2e^- \rightarrow 2H_2 \quad (9)$$

3.2.2. Effect of catalyst loading

The experiment was carried out with different amounts of catalyst (0.05 g/L, 0.1 g/L and 0.2

g/L). As illustrated in figure 6, decreasing the catalyst dosage from 0.1 g/L to 0.5 g/L, the MO removal efficiency decreased from 92.94% to 85.18% (120 min of reaction). The results also indicated that the MO removal efficiency with $MnFe_2O_4$/C was significantly higher than that without the catalyst (0.00 g/L), where the maximum removal efficiency was only about 67%. This can be explained by the limited limitation of active sites on the catalyst surface, leading to the limited formation of free hydroxyl radicals •OH according to equations (4) and (5). When the amount of catalyst increased to 0.2 g/L, the MO removal efficiency recorded in the first 15 min (36.28%) was higher than that in the catalyst condition of 0.1 g/L (27.23%), due to the combination of electrochemical oxidation and adsorption (more material content, higher adsorption capacity). However, after 30 min of reaction, the MO removal efficiency with the catalyst loading of 0.2 g/l was lower than that in the condition of 0.1 g/L (slightly decreased from 92.94% to 90.1%) due to the scavenging effect of Fe^{II}, which inactivated the •OH radical according to equation (10) [20].

$$Fe^{II} + \bullet OH \rightarrow Fe^{III} + OH^- \quad (10)$$

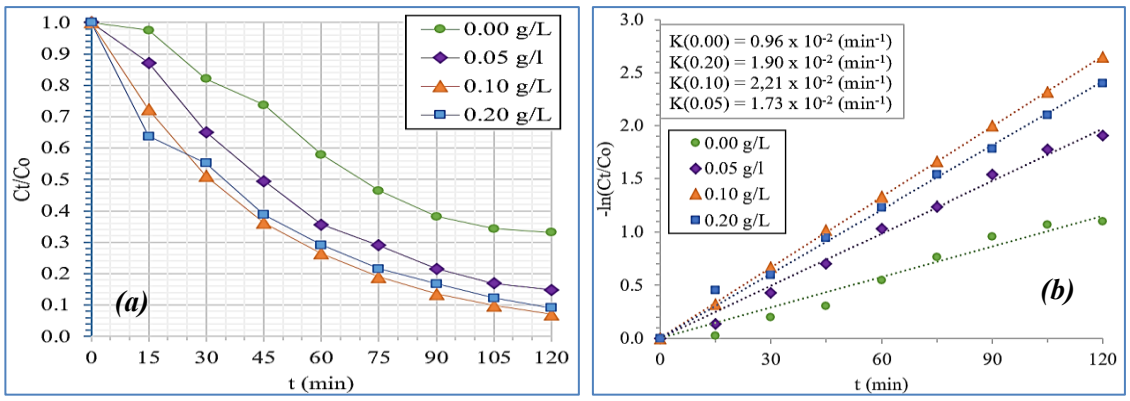

Figure 6. *Effect of catalyst loading; conditions: initial MO concentration 100 ppm, current density 3 mA/cm², Na_2SO_4 electrolyte 0.0025 mol/L.*

3.2.3. Effect of initial methyl orange concentrations

The effect of the initial MO concentration was investigated from 50 ppm to 400 ppm. The results are presented in figure 7. It can be seen that the MO removal efficiency decreased slightly when increasing the initial MO concentration. The apparent rate constants (K) corresponding to initial MO concentrations of 100 ppm, 200 ppm, 400 ppm were 2.21 x 10^{-2} (min^{-1}), 1.72 x 10^{-2} (min^{-1}), 1.54 x 10^{-2} (min^{-1}). The decrease in removal of MO with an increase in concentration can be ascribed to the lesser number of available •OH for the oxidation [10].

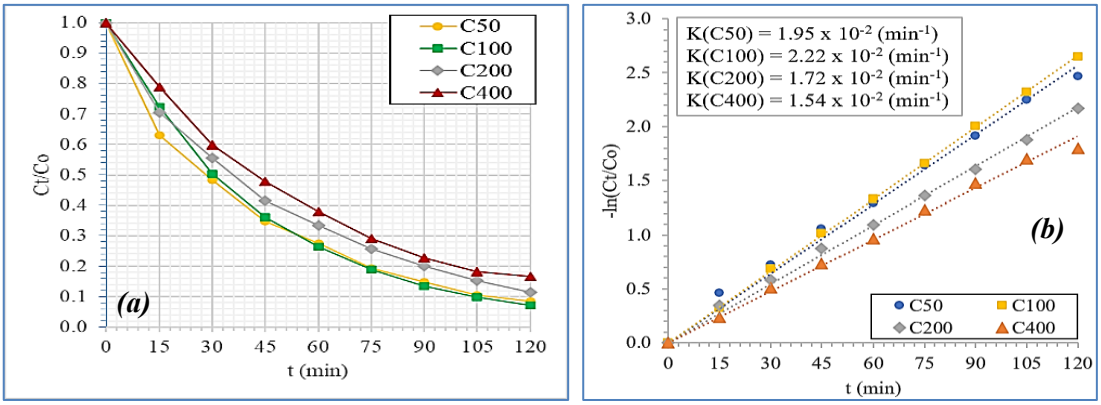

Figure 7. *Effect of the initial MO; conditions: current density 3 mA/cm², Na_2SO_4 electrolyte 0.0025 mol/L, $MnFe_2O_4$/C 0.1 g/L.*

On the other hand, the efficiency of MO removal was basically the same with initial MO concentrations of 50 ppm and 100 ppm. This phenomenon may be due to the low MO concentration in the solution reducing the probability of oxidation at the active site of the catalyst during the reaction progress. The apparent rate constant (K) of 50 ppm only achieved 1,95 x 10^{-2} (min^{-1}), which was lower than the initial MO concentration of 100 ppm. This shows that the best efficiency of pollutant removal occurs at a certain ratio of catalyst/pollutant. When this ratio is high, it will lead to a decrease in the pollutant removal rate due to the scavenging of hydroxyl radical according to equation (10).

3.2.4. Effect of initial pH

The experimental results indicated that the highest MO removal efficiency was obtained at pH = 3, reaching 95.6% with an apparent rate constant of k = 2.57 × 10^{-2} min^{-1}. At pH = 9, the efficiency decreased significantly, achieving only 86% with a lower apparent rate constant (k = 1.66 × 10^{-2} min^{-1}). At near-neutral conditions (pH ≈ 7), the removal efficiency slightly decreased compared to pH = 3, but still achieved high efficiency (92.94%) with an apparent rate constant of k = 2.21 × 10^{-2} min^{-1}. These results are consistent with previously reported studies and highlight the advantage of the heterogeneous electro-Fenton process, which exhibits a wider effective pH range compared to conventional Fenton systems.

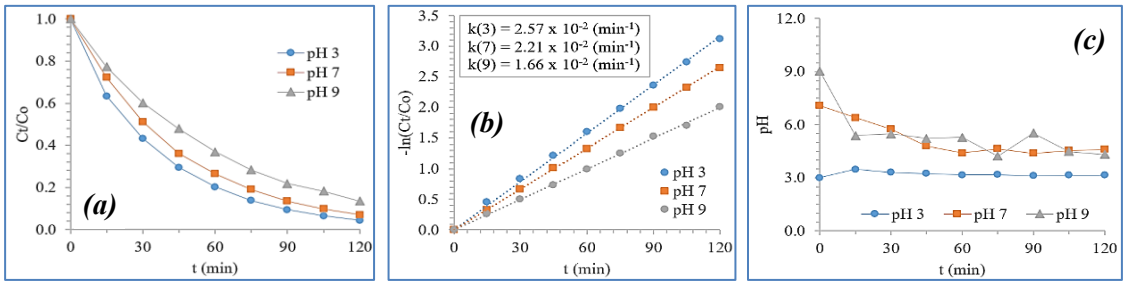

Figure 8. *Effect of initial pH (a), (b) and trend of pH changing (c). Conditions: initial MO=100 ppm, current density 3 mA/cm², Na_2SO_4 electrolyte 0.0025 mol/L, $MnFe_2O_4$/C 0.1 g/L.*

In addition, the results revealed clear trends in pH variation during the heterogeneous electro-Fenton process under both acidic and alkaline initial conditions. At an initial pH of 3, the pH value remained nearly constant throughout the reaction. In contrast, at initial pH values of 7 and 9, the solution pH gradually decreased and stabilized at approximately 4.8 ± 0.2. This phenomenon may be attributed to the formation of intermediate products, particularly low-molecular-weight organic acids such as acetic, oxalic, and formic acids. On the other hand, these findings can also be interpreted as indicating that the pH self-adjustment ability is due to the favorable reaction environment of the heterogeneous electro-Fenton process with $MnFe_2O_4$/C catalyst material.

3.2.5. Catalyst reusability examination

The reusability of the catalyst is an important advantage of the heterogeneous electro-Fenton. The catalyst should have the ability to be separated from the effluent easily and reused several times without activity loss. Therefore, the long-term stability of the catalyst is quite important.

To evaluate the reusability of the $MnFe_2O_4$/C catalyst, experiments were conducted over four reuse cycles. After each cycle, the material was separated from the solution using a magnet and then reused in the subsequent cycle. The results in figure 9 showed that the treatment efficiency remained high after 120 minutes (about 90 - 92% for all cycles). However, the treatment efficiency and the MO removal rate constant were slightly lower in later cycles during the 30–90 minute period. This is consistent with the observation that the catalyst experienced a slight decrease in activity after each use, although the decline was not significant. These findings confirm the practical application potential of the catalyst in wastewater treatment via the heterogeneous electro-Fenton process.

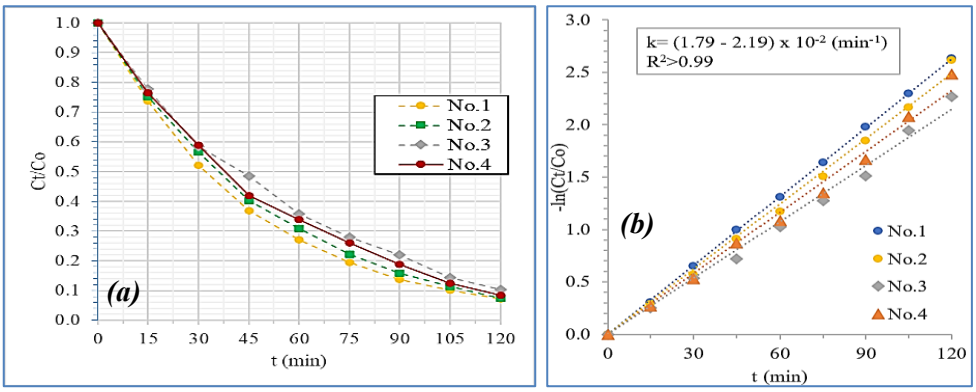

Figure 9. *The reusability of $MnFe_2O_4$/C material.*

4. CONCLUSIONS

The study results indicate that carbon-supported manganese ferrite ($MnFe_2O_4$/C) was successfully synthesized using the impregnation-coprecipitation method. The degradation of methyl orange using the electro-Fenton process with the $MnFe_2O_4$/C catalyst achieved a high efficiency of 92.94% under neutral pH (pH in the range of 6.8–7.08) with various optimized parameters such as a current density of 3 mA/cm², a catalyst loading of 0.1 g/L, and an initial methyl orange concentration of 100 ppm. The kinetics of the degradation reaction follow the pseudofirst-order kinetics model ($k = 2.21 \times 10^{-2}$ min^{-1}, $R^2 = 0{,}9996$). The reusability of material was also examined, the removal efficiency still reached approximately 92% (120 min reaction) after four reuse cycles. This study highlights the potential of the heterogeneous Electro-Fenton process for the treatment of persistent organic compounds using the $MnFe_2O_4$/C catalyst.

Acknowledgment: *This research was supported by the Academy of Military Science and Technology.*

REFERENCES

[1]. Kumar D.S. et al., *"Removal of toxic methyl orange by a cost-free and eco-friendly adsorbent: Mechanism, phytotoxicity, thermodynamics, and kinetics"*, South African Journal of Chemical Engineering, Vol. 40, pp. 195–208, (2022).

[2]. H. Jiang et al., *"Heterogeneous electro-Fenton oxidation of azo dye methyl orange catalyzed by magnetic Fe3O4 nanoparticles"*, Water Science and Technology, Vol. 74, No. 5, pp. 1116–1126, (2016).

[3]. Denga Ramutshatsha-Makhwedzha et al., *"Activated carbon derived from waste orange and lemon peels for the adsorption of methyl orange and methylene blue dyes from wastewater"*, Heliyon, Vol. 8, No. 8, (2022).

[4]. Farhan H.M. and Norzahir S., *"A review on the water problem associated with organic pollutants derived from phenol, methyl orange, and remazol brilliant blue dyes"*, Materials Today: Proceedings, Vol. 31, pp. A141–A150, (2020).

[5]. Arwa Alseddig Ahmed Eljiedi and Azlan Kamari, *"Removal of methyl orange and methylene blue dyes from aqueous solution using lala clam (Orbicularia orbiculata) shell"*, AIP Conference Proceedings, AIP Publishing LLC, (2017).

[6]. Fortunate Phenyo Sejie and Misael Silas Nadiye-Tabbiruka, *"Removal of methyl orange (MO) from water by adsorption onto modified local clay (kaolinite)"*, Physical Chemistry, Vol. 6, No. 2, pp. 39–48, (2016).

[7]. Iwuozor K.O. et al., *"Adsorption of methyl orange: A review on adsorbent performance"*, Current Research in Green and Sustainable Chemistry, Vol. 4, p. 100179, (2021).

[8]. Sifani Z. et al., *"Degradation of organic methyl orange (MO) dye using a photocatalyzed non-ferrous Fenton reaction"*, Nanomaterials, Vol. 13, No. 4, p. 639, (2023).

[9]. Macarena Munoz et al., *"Preparation of magnetite-based catalysts and their application in heterogeneous Fenton oxidation – a review"*, Applied Catalysis B: Environmental, Vol. 176, pp. 249–265, (2015).

[10]. G. Anil, J. Scaria, Nidheesh P.V., *"Removal of synthetic dye from aqueous solution using MnFe2O4–GO catalyzed heterogeneous electro-Fenton process"*, Water, Vol. 14, p. 3350, (2022).
[11]. Fahma Riyanti et al., *"The synthesis of MnFe2O4–activated carbon composite for removal of methyl red from aqueous solution"*, Molekul, Vol. 13, No. 2, pp. 123–132, (2018).
[12]. Z. Wan, J. Wang, *"Degradation of sulfamethazine using Fe3O4–Mn3O4/reduced graphene oxide hybrid as Fenton-like catalyst"*, Journal of Hazardous Materials, Vol. 324, pp. 653–664, (2017).
[13]. Agus Rimus Liandi et al., *"Recent trends of spinel ferrites (MFe2O4: Mn, Co, Ni, Cu, Zn) applications as an environmentally friendly catalyst in multicomponent reactions: A review"*, Case Studies in Chemical and Environmental Engineering, Vol. 7, p. 100303, (2023).
[14]. M.M. Cruz et al., *"Enhanced magnetic hyperthermia of CoFe2O4 and MnFe2O4 nanoparticles"*, Journal of Alloys and Compounds, Vol. 703, pp. 370–380, (2017).
[15]. Minghua Zhou, Mehmet A. Oturan, and Ignasi Sires, *"Electro-Fenton Process"*, Springer, (2018).
[16]. Qiang L. et al., *"Degrade methyl orange by a reverse electrodialysis reactor coupled with electrochemical direct oxidation and electro-Fenton processes"*, Electrocatalysis, Vol. 13, No. 3, pp. 242–254, (2022).
[17]. Cui Lai et al., *"Fabrication of novel magnetic MnFe2O4/bio-char composite and heterogeneous photo-Fenton degradation of tetracycline in near neutral pH"*, Chemosphere, Vol. 224, pp. 910–921, (2019).
[18]. Thi Dung Nguyen et al., *"Magnetic Fe2MO4 (M: Fe, Mn) activated carbons: fabrication, characterization and heterogeneous Fenton oxidation of methyl orange"*, Journal of Hazardous Materials, Vol. 185, No. 2–3, pp. 653–661, (2011).
[19]. Jessica Meijide et al., *"Heterogeneous electro-Fenton as 'Green' technology for pharmaceutical removal: A review"*, Catalysts, Vol. 11, No. 1, p. 85, (2021).
[20]. Pegah Nazari, Neda Askari, and Shahrbanoo Rahman Setayesh, *"Oxidation-precipitation of magnetic Fe3O4/AC nanocomposite as a heterogeneous catalyst for electro-Fenton treatment"*, Chemical Engineering Communications, Vol. 207, No. 5, pp. 665–675, (2020).

TÓM TẮT

Nghiên cứu loại bỏ methyl orange bằng quá trình Fenton điện hóa dị thể, sử dụng vật liệu xúc tác $MnFe_2O_4$/C

Trong nghiên cứu này, quá trình Fenton điện hóa dị thể sử dụng xúc tác manganese trên than hoạt tính có nguồn gốc từ bã mía ($MnFe_2O_4$/C) để loại bỏ thuốc nhuộm methyl orange trong nước thải mô phỏng. $MnFe_2O_4$/C được tổng hợp bằng phương pháp tẩm-đồng kết tủa và được xác định các đặc tính bằng kính hiển vi điện tử quét (SEM), phổ kế tia X tán xạ năng lượng (EDS), nhiễu xạ tia X (XRD). Mô hình Fenton điện hóa sử dụng điện cực than chì được áp dụng để thử nghiệm đánh giá hiệu quả loại bỏ methyl orange trong điều kiện pH trung tính. Ảnh hưởng của các yếu tố khác nhau như dòng điện sử dụng, hàm lượng chất xúc tác, nồng độ methyl orange ban đầu đã được nghiên cứu.

Từ khóa: Fenton điện hóa dị thể; Methyl orange; Manganese ferrite; Than bã bía; $MnFe_2O_4$/C.